Proceedings of the 1st Global Power and Propulsion Forum
GPPF 2017
Jan 16-18, 2014, Zurich, Switzerland
www.pps.global

GPPF-2017-116

MULTI-OBJECTIVE DESIGN OPTIMIZATION OF A DERIVATIVE THREE-SPOOL ULTRA-HIGH BYPASS DIRECT DRIVE TURBOFAN ENGINE USING NON-DOMINATED SORTING GENETIC ALGORITHM-II

Sangmin Lee
Siemens Energy Inc.,
neysonlee@gmail.com
Houston, TX, USA

ABSTRACT

There have been escalated demands of advanced technologies for subsonic commercial aircraft engines that can enable economic long range travels with reduced fuel consumption. To accommodate the demands, numerous studies have been performed for the last several decades to develop various advanced aircraft engines, figuring out that implementing ultra-high bypass turbofan engines are superior to the established engines regarding fuel and propulsive efficiency. However, developing a new engine from scratch is technically challenging and guzzles resources so that many advanced engines are devised by a derivation from existing ones. In this perspective, this paper proposes a cycle design optimization methodology for the development of a derivative three-spool Ultra-High Bypass Direct Drive Separate Flow (UHB DDSF) turbofan engine retaining the HP system of a turbofan engine existing in the market. The engine cycle analysis for a generic turbofan engine is conducted in a multi-objective design optimization (MODO) environment in ModelCenter and the result is validated with GasTurb 12, a popular tool for gas turbine performance simulations. A parametric trade-off study among the important design variables is also carried out with the model to provide the detailed information of how the design variables are interrelated. This model is based on Non-Dominated Sorting Genetic Algorithm, NSGA-II, that to rapidly obtain the global minimum of the specific fuel consumption (SFC) and the engine diameter regarding air mass flow rate under pre-determined constraints. The design optimization environment yields the optimum cycle configurations of a derivative three-spool UHB DDSF turbofan engine and the relative significance of the design variables.

INTRODUCTION

Developing subsonic commercial aircraft engines with better performance has been one of the main engineering concerns in the history. To achieve this goal, the latest technological paradigm shift took place in around 1980s by the advent of 'turbo' engines such as turbojet, turbofan, turboprop, etc. After that, numerous engine scientists have been committed to improving the performance of engines regarding specific fuel consumption. Throughout these endeavors, a variety of derivative turbo engines has been designed and manufactured.

However, developing an engine is a very complex system-of-systems engineering (SoSE) which inevitably involves state-of-the-art technologies. Due to this complexity, developing a new engine from scratch is technically challenging, painstaking and guzzles a vast amount of resources. For this reason, it is advantageous to devise a new engine by modifying established design variables to satisfy the goals defined. In this perspective, a framework for engine cycle optimization has been built which can formulate the goal of minimizing thrust specific fuel consumptions and the engine diameter.

The developed design optimization framework seeks to design a derivative three-spool UHB DDSF turbofan engine retaining the HP system of a turbofan engine existing in the market. The HP system is chosen to be retained because it is considered as the most time consuming and costly part of new engine developments due to the high temperature and pressure conditions.

For engine cycle analysis, a MatLab code is firstly developed for a baseline engine and a generic turbofan engine data is used to validate the code with a set of results from GasTurb 12. This model embraces critical design variables associated with the aimed engine and is incorporated into ModelCenter, a comprehensive engineering design optimization solution to form the multi-objective design optimization framework.

A genetic algorithm (NSGA-II) is then implemented to rapidly obtain the global minimum of the thrust specific fuel

consumption (TSFC) and engine diameter in terms of air mass flow rate under pre-determined constraints.

The design optimization environment eventually yields the optimum design configurations of a UHB DDSF turbofan engine. During this process, various parametric studies are also conducted to retrieve the interrelationships between design variables and outputs.

.

METHODOLOGY

Review of parametric cycle analysis of three-spool separate flow turbofan engines

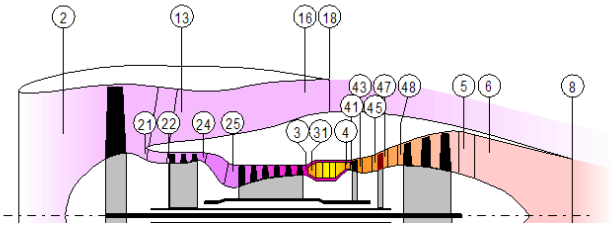

Figure 1 Engine Station Numbering

The parametric cycle analysis begins with the calculations of several basic physical parameters as follows based on the given inputs.

$$R_c = \frac{(\gamma_c - 1)}{\gamma_c} c_{pc} \quad (1)$$

$$R_t = \frac{(\gamma_t - 1)}{\gamma_t} c_{pt} \quad (2)$$

$$a_0 = \sqrt{\gamma_c \times R_c \times T_0} \quad (3)$$

$$V_0 = a_0 \times M_0 \quad (4)$$

$$\tau_\lambda = \frac{c_{pt} T_{t4}}{c_{pc} T_{00}} \quad (5)$$

$$\tau_r = 1 + \frac{(\gamma_c - 1)}{2} M_0^2 \quad (6)$$

$$\pi_r = \tau_r^{\gamma_c/(\gamma_c - 1)} \quad (7)$$

$$\pi_d = \pi_{dmax} \times \eta_r \quad (8)$$

Where, τ and π are the convenient form of the ratios of total pressures and temperatures across a component and these can be expressed as

$$\pi_a = \frac{total\ pressure\ leaving\ component\ a}{total\ pressure\ entering\ component\ a} \quad (9)$$

$$\tau_a = \frac{total\ temperature\ leaving\ component\ a}{total\ temperature\ entering\ component\ a} \quad (10)$$

The temperature and pressure changes through the inlet duct are

$$P_{t2} = P_0 \times \pi_d \quad (11)$$

$$T_{t2} = T_0 \times \pi_d^{0.3175} \quad (12)$$

Through the fan

$$\tau_f = FPR^{\frac{\gamma_c - 1}{\gamma_c e_f}} \quad (13)$$

$$P_{t21} = FPR \times P_{t2} \quad (14)$$

$$T_{t21} = \tau_f T_{t2} \quad (15)$$

$$\eta_f = \frac{FPR^{\frac{(\gamma_c - 1)}{\gamma_c}} - 1}{\tau_f - 1} \quad (16)$$

Because this model is designed to deal with a derivative turbofan engine retaining the HP compressor and turbine of the baseline engine, it is a reasonable assumption that the area ratio of the HP compressor inlet and outlet remains the same as the baseline engine. By assuming that the axial airflow velocity is approximately constant and the mass is conserved through the HP compressor,

$$\rho_{t_{25}} A_{t_{25}} \approx \rho_{t_3} A_{t_3} \quad (17)$$

$$A_{hpc} = \frac{A_{t25}}{A_{t3}} \approx \left(\frac{P_{t3}}{P_{t25}}\right)^{\frac{1 - \gamma_c(1 - e_c)}{\gamma_c e_c}} \quad (18)$$

Equation (18) can be recast as

$$P_{t25} = \frac{P_{t3}}{A_{hpc}^{\frac{1}{\gamma_c e_{hpc}} \frac{1}{1 - \gamma_c(1 - e_{hpc})}}} \quad (19)$$

The compressor outlet pressure is calculated with the given compress ratio as

$$P_{t3} = \pi_c P_{t2} \quad (20)$$

moreover, the thermodynamic relationships for the IP compressor are given by

$$\pi_{ipc} = \frac{P_{t25}}{P_{t21}} \quad (21)$$

$$\tau_{ipc} = \pi_{ipc}^{\frac{\gamma_c - 1}{\gamma_c e_{ipc}}} \quad (22)$$

$$T_{t24} = \tau_{ipc} T_{t21} \quad (23)$$

$$\eta_{ipc} = \frac{\pi_{ipc}^{\frac{(\gamma_c - 1)}{\gamma_c}} - 1}{\tau_{ipc} - 1} \quad (24)$$

Similarly, for the HP compressor,

$$\pi_{hpc} = \frac{P_{t3}}{P_{t25}} \quad (25)$$

$$\tau_{hpc} = \tau_{ipc}^{\frac{\gamma_c - 1}{\gamma_c e_{hpc}}} \quad (26)$$

$$T_{t25} = T_{t24} \quad (27)$$

$$T_{t3} = \tau_{hpc} T_{t25} \quad (28)$$

$$\eta_{hpc} = \frac{\pi_{hpc}^{\frac{(\gamma_c - 1)}{\gamma_c}} - 1}{\tau_{hpc} - 1} \quad (29)$$

Now the temperature ratio and efficiency of the entire compressor can be obtained as

$$\tau_c = \frac{T_{t3}}{T_{t2}} \tag{30}$$

$$\eta_c = \frac{\pi_c^{\frac{(\gamma_c-1)}{\gamma_c}}-1}{\tau_c-1} \tag{31}$$

Moreover, we can find the fuel/air ratio in the convenient form with the given burner efficiency.

$$f = \frac{\tau_\lambda - \tau_r\tau_c}{\frac{h_{fuel}\eta_b}{c_p T_{t2}} - \tau_\lambda} \tag{32}$$

Taking into account the power balance between the HP turbine and HP compressor together with a mechanical efficiency, the HP turbine outlet temperature is given by

$$T_{t43} = T_{t4} - \frac{c_{pc}(T_{t3}-T_{t24})}{c_{pt}\eta_{mhp}(1+f)} \tag{33}$$

and the rest of the thermodynamic properties can be expressed as follows.

$$P_{t4} = \pi_b P_{t3} \tag{34}$$

$$\tau_{hpt} = \frac{T_{t43}}{T_{t4}} \tag{35}$$

$$\pi_{hpt} = \tau_{hpt}^{\frac{\gamma_t e_{hpt}}{\gamma_t-1}} \tag{36}$$

$$P_{t43} = \pi_{hpt} P_{t4} \tag{37}$$

$$\eta_{hpt} = \frac{1-\tau_{hpt}}{1-\tau_{hpt}^{1/e_{hpt}}} \tag{38}$$

Proceeding as in the HP turbine case, we find the IP and LP turbine details.

IP turbine:

$$T_{t45} = T_{t43} \tag{39}$$

$$T_{t47} = T_{t45} - \frac{c_{pc}(T_{t24}-T_{t21})}{c_{pt}\eta_{mip}(1+f)} \tag{40}$$

$$\tau_{ipt} = \frac{T_{t47}}{T_{t45}} \tag{41}$$

$$\pi_{ipt} = \tau_{ipt}^{\frac{\gamma_t e_{ipt}}{\gamma_t-1}} \tag{42}$$

$$P_{t47} = P_{t43}\pi_{ipt} \tag{43}$$

$$\eta_{ipt} = \frac{1-\tau_{ipt}}{1-\tau_{ipt}^{1/e_{ipt}}} \tag{44}$$

LP turbine:

$$T_{t45} = T_{t43} \tag{45}$$

$$T_{t5} = T_{t47} - BPR\frac{c_{pc}(T_{t21}-T_{t2})}{c_{pt}\eta_{mlp}(1+f)} \tag{46}$$

$$\tau_{lpt} = \frac{T_{t5}}{T_{t47}} \tag{47}$$

$$\pi_{lpt} = \tau_{lpt}^{\frac{\gamma_t e_{lpt}}{\gamma_t-1}} \tag{48}$$

$$P_{t5} = P_{t47}\pi_{lpt} \tag{49}$$

$$\eta_{lpt} = \frac{1-\tau_{lpt}}{1-\tau_{lpt}^{1/e_{lpt}}} \tag{50}$$

Recognizing that P_{t5}/P_{tc} is the critical pressure ratio in the core nozzle for choking condition,

$$\frac{P_{t5}}{P_{tc}} = \frac{1}{\left[1-\frac{\gamma_t-1}{\eta_{cn}(\gamma_t+1)}\right]^{\frac{\gamma_t}{\gamma_t-1}}} \tag{51}$$

$$\pi_{cn} = \frac{P_{t5}}{P_0} \tag{52}$$

The core nozzle is choked when $P_{t5}/P_{tc} \le \pi_{cn}$ and hence,

$$P_8 = P_{tc} \tag{53}$$

$$T_{t5} - T_8 = \eta_{cn}T_{t5}\left[1-\left(\frac{1}{P_{t5}/P_{tc}}\right)^{\frac{\gamma_t-1}{\gamma_t}}\right] \tag{54}$$

$$V_8 = \sqrt{2c_{pt}(T_{t5}-T_8)} \tag{55}$$

If the core nozzle is not choked

$$P_8 = P_0 \tag{56}$$

$$T_{t5} - T_8 = \eta_{cn}T_{t5}\left[1-\left(\frac{1}{P_{t5}/P_0}\right)^{\frac{\gamma_t-1}{\gamma_t}}\right] \tag{57}$$

$$V_8 = \sqrt{2c_{pt}(T_{t5}-T_8)} \tag{58}$$

Similarly, the critical pressure ratio in the fan nozzle is given by,

$$\frac{P_{21}}{P_{fc}} = \frac{1}{\left[1-\frac{\gamma_c-1}{\eta_{fn}(\gamma_c+1)}\right]^{\frac{\gamma_c}{\gamma_c-1}}} \tag{59}$$

The fan nozzle is under choking condition if $P_{21}/P_{fc} \le FPR$, therefore,

$$P_{18} = P_{fc} \tag{60}$$

$$T_{t21} - T_{18} = \eta_{fn}T_{t21}\left[1-\left(\frac{1}{FPR}\right)^{\frac{\gamma_c-1}{\gamma_c}}\right] \tag{61}$$

$$V_{18} = \sqrt{2c_{pc}(T_{t21}-T_{18})} \tag{62}$$

If the fan nozzle is not choked,

$$P_{18} = P_0 \tag{63}$$

$$T_{t21} - T_{18} = \eta_{fn}T_{t21}\left[1-\left(\frac{1}{P_{t21}/P_0}\right)^{\frac{\gamma_c-1}{\gamma_c}}\right] \tag{64}$$

$$V_{18} = \sqrt{2c_{pc}(T_{t21}-T_{18})} \tag{65}$$

Now we have the familiar expressions for the thrust forces of the fan and core respectively,

$$F_f = BPR\frac{\dot{m}_{air}V_{18}}{(BPR+1)} \quad (66)$$

$$F_c = \frac{(1+f)\dot{m}_{air}V_8}{(BPR+1)} \quad (67)$$

The total thrust is then given by,

$$F_n = F_f + F_c \quad (68)$$

The net thrust specific fuel consumption is also defined in terms of F_n as

$$TSFC = \dot{m}_{fuel}/F_n \quad (69)$$

Baseline Engine Model

A three-spool turbofan engine model is coded in MatLab to be used as the core part of the ModelCenter based on the theory introduced in the previous section. With the given inputs, it calculates the pressure and temperature changes from the inlet duct through the engine exhaust. These changes indeed produce desired engine performance like thrust and specific fuel consumption as well as other interested engine parameters.

Because this study deals with derivative engine cycle development, the baseline engine model is designed to retain the HP system of an existing engine. However, this model is 0-dimensional and considers neither the turbomachinery design nor engine geometries. To overcome this obstacle, equation (18) is implemented in the code and fixed during the parametric analysis. This method is not complete but logical because the area ratio of HP compressor inlet and outlet approximated by equation (18) is strongly related to the system geometry. This limits the upstream compressor parameters with the given overall compress ratio (π_c) and eventually proposes how the LP and IP parts of the engine need to be modified to achieve the desired engine performance in a derivative engine.

Optimization Algorithm

Non-dominated Sorting Genetic Algorithm II (NSGA-II), which is provided as an option in ModelCenter, is selected for its advantages on the multi-objective optimizations. This algorithm is known to overcome the major difficulties of multi-objective evolutionary algorithms (MOEAs) by reducing the computational complexity, utilizing elitism, and specifying a sharing parameter. On the basis of these advantages, this algorithm has shown its advanced performance in numerous studies finding a better spread of solutions and convergence near the true Pareto-optimal front.

To that end, there seems to be no compelling reason to argue that this algorithm provides genuine fit for this study; Optimization provisioning minimizations of both TSFC and engine diameter (in terms of air mass flow rate) with respect to multiple constraints by changing dominant engine design variables.

Design and Optimization Environment (ModelCenter)

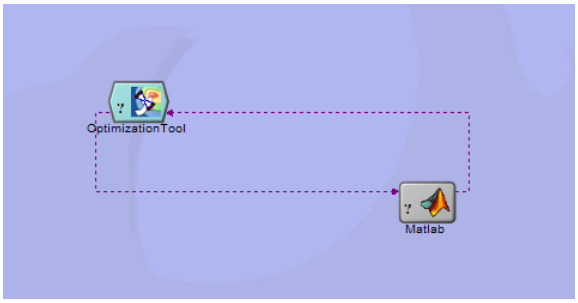

Figure 2 Schematic Diagram of ModelCenter

ModelCenter is popular software that enables model-based engineering simulation environment. The basic concept of this software is to integrate various engineering tools and create seamless workflows among those for multidisciplinary and multi-objective simulations and optimizations. One great additional advantage of ModelCenter is that it also provides various data analysis tools such as DoE and multiple plotting options for sensitivity and feasibility studies.

In this study, the baseline engine model coded in MatLab is implemented here along with an optimization tool, NSGA-II, in anticipation of seamless workflows of multi-objective engine optimizations.

RESULTS AND DISCUSSION

Validation of Baseline Engine

Table 1 Baseline Engine Basic Input (SLS)

Property	Unit	Value
Intake Pressure Ratio		1
Fan Pressure Ratio, *FPR*		1.4
IP Compressor Ratio, π_{ipc}		6.3
HP Compressor Ratio, π_{hpc}		5.76
Overall Compressor Ratio, π_c		50
Air Flow Rate, $\dot{m}_{air}$	kg/s	1442.92
Burner Exit Temperature, T_{t4}	K	1783.3
Burner Design Efficiency, η_b		0.9995
Design Bypass Ratio, *BPR*		9.3
Fuel Heating Value, h_{fuel}	MJ/kg	43.124
HP Spool Mechanical Efficiency, η_{mhp}		0.99
IP Spool Mechanical Efficiency, η_{mip}		0.999
LP Spool Mechanical Efficiency, η_{mlp}		0.999
Burner Pressure Ratio, π_b		0.96
HP Area Ratio, A_{hpc}		3.38*

*An input only for the engine code(MatLab)

The coded baseline model is validated with GasTurb by publically available engine data in Reference [1]. With the inputs in Table 1, the temperature/pressure changes and two other interested engine performance factors are calculated. Figure 4 and 5 reveal that the pressure and temperature at each engine station match those from GasTurb. One point to be noted is that, unlike GasTurb, the engine code does not account for the pressure/temperature changes through the internal engine structures in between the spools. Moreover, this is the reason why the pressures of the engine code are higher on the turbine stations within an acceptable range (~5%) than those of GasTurb.

As shown in Table 2, the calculated engine thrust force (FN) and thrust specific fuel consumption (TSFC) are in good agreement too. The FN of the engine code is 3.2% higher than that of GasTurb due to the higher core exit velocity. This higher exit velocity is attributable to the relatively higher temperature changes through the exhaust nozzle.

Table 2 Baseline Engine Output (SLS)

	Unit	GasTurb	Engine Code (MatLab)	Error (%)
FN	*kN*	400.26	413.79	3.2
$TSFC$	*g/(kN s)*	8.04	8.05	0.1

Optimization of Derivative Engine (UHB DDSF Turbofan Engine)

In this section, a UHB DDSF turbofan engine is developed via multi-objective optimization. The developed design and optimization model in ModelCenter is utilized to minimize both TSFC and engine diameter regarding air mass flow rate. The following is the optimization problem statement.

Min: $\{TSFC,\ \dot{m}_{air}\}$
By changing: $\{\pi_c,\ FPR,\ T_{t4}, BPR\}$
Subject to: $\{T_{t3},\ T_{t4},\ T_{t5},\ \dot{m}_{air}\}$

The upper and lower bound of the design variables and constraints are organized in Table 3 and 4 respectively.

Table 3 Design Variables

	Lower Bound	Upper Bound	Unit
π_c	40	60	
FPR	1	1.6	
T_{t4}	1700	1930	*K*
BPR	12	18	

The bounds of the design variables aiming at the requirements in reference [1] are set up at the acceptable range for desired UHB DDSF turbofan engines.

Likewise, the constraints are based on the technology level that will become available shortly. T_{t4} is increased to 1930K assuming that advances in material and cooling technology permit this temperature. T_{t3} is limited at 1000K accounting for the material cost. Especially, the upper bound of $\dot{m}_{air}$ is set anticipating being minimized under 1500 kg/s, which is 5% larger than the baseline. Because this study is an attempt to develop a derivative engine that retains the HP system of the original engine, increasing BPR can be done by either enlarging the bypass duct area or redesigning the IP and LP parts of the engine or both on logical grounds. In any cases, the ultimate goal of this study is to develop a derivative engine, which can be installed on the original aircraft or similar size aircraft. Along this line and considering the fact that air mass flow rate is well correlated to the engine diameter, limiting the air mass flow rate at around the original engine value is considered as reasonable assumption.

Table 4 Constraints

	Lower Bound	Upper Bound	Unit
T_{t3}	-	1000	*K*
T_{t4}	-	1930	*K*
T_{t5}	800	-	*K*
$\dot{m}_{air}$	-	1500	*kg/s*

The algorithm options used for this study are shown below in Table 5. The number of population and the max generations are adjusted accounting for the number of variables, constraints, and computation time.

Figure 3 illustrates the number of runs and the convergence behavior of the algorithm for the two objective functions. As expected, the performance of the algorithm is superior. The model starts converging after around 50 runs. For the remaining runs, the model keeps converging to seek the optimum values in narrow ranges while meeting all the predetermined constraints and finally finds the global minimum of the two objective functions after 757th run.

Table 5 NSGA-II Options

Optimization Parameters	
Population	28
Optimization Parameters for Binary Variables	
Binary Cross Over Probability	0.7
Binary Mutation Probability	0.5
Optimization Parameters for Real Variables	
Crossover Probability	0.7
EtaC	15
EtaM	20
Mutation Probability	0.2
Stopping Criteria	
Conversions Generations	5
Conversions Threshold	0.001
Max Evaluations	2000
Max Generations	100

The optimized UHB DDSF turbofan engine properties are gathered in Table 6. Significant improvement is observed in TSFC (21.2%) comparing to the baseline engine. This improvement is accomplished mainly by increasing BPR (59.1%) while maintaining the engine thrust force and the HP system. Interestingly, this improvement does not change the air mass flow rate (+0.8%) at a noticeable rate thus; it can be

assumed that no change is required in the engine diameter. Notwithstanding minor changes are observed in the IP system, the fan pressure ratio is increased by 5%.

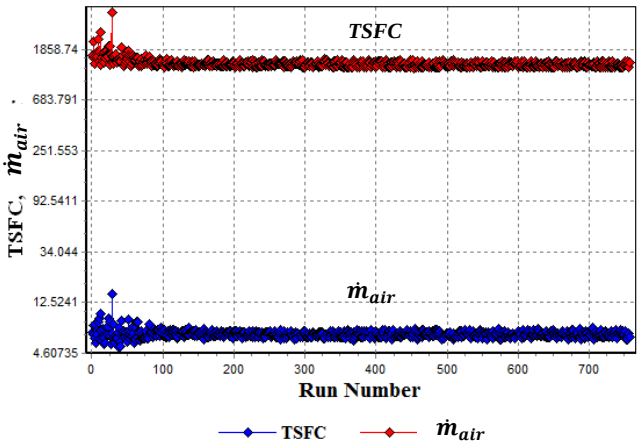

Figure 3 Line Chart of Optimization Performance

The engine parameters of the developed UHB engine are put into GasTurb for validation. Figure 4 and 5 compare the pressure and temperature changes and show those are in good agreement. Higher temperatures and pressures are observed comparing to the baseline engine. Table 6 shows the engine model in ModelCenter predicts 7.3% lower TSFC, but this seems reasonable considering GasTurb's better accuracy level.

Table 6 Engine Property of UHB DDSF Turbofan Engine

Property	Unit	Value	% Change
Fan Pressure Ratio, *FPR*		1.47	+5.0
IP Compressor Ratio, π_{ipc}		6.2	-1.5
HP Compressor Ratio, π_{hpc}		5.73	-0.5
Overall Compressor Ratio, π_c		52.6	+5.2
Burner Exit Temperature, T_{t4}	*K*	1921.19	+7.7
Bypass Ratio, *BPR*		14.8	+59.1
HP Area Ratio, A_{hpc}		3.38	-
Fuel Air Ratio, f		0.0304	+13.9
FN	*kN*	400.5	-3.2
TSFC	*g/(kN s)*	6.34	-21.2
Air Flow Rate, $\dot{m}$	*kg/s*	1454.8	+0.8

Parametric and Sensitivity Study on the developed UHB DDSF Turbofan Engine

Figure 6 is a scatter plot of TSFC and BPR. It reveals that there is a strong negative relationship between TSFC and BPR and this fact supports the reason why TSFC decreases as BPR increases. In addition, a close look at the data indicates that the increasing π_c doesn't always guarantee the improvement of TSFC if π_c is higher than certain level. Based on the population on the frontier front in Figure 6, the number of green dots implies that the inflection point of π_c is located around 50 in regards to TSFC. Grey dots are outliers of π_c.

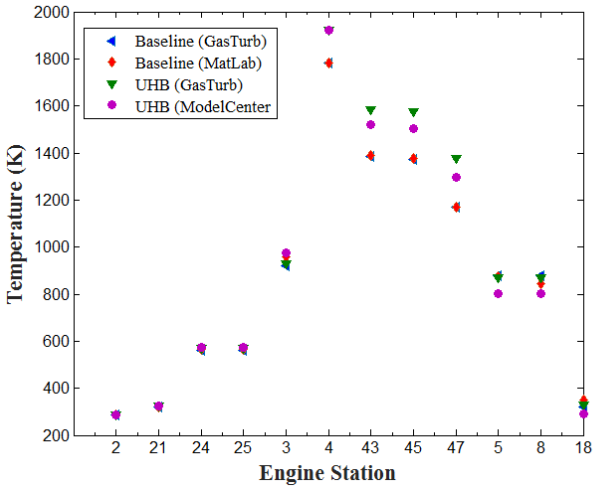

Figure 4 Temperatures @ Engine Stations

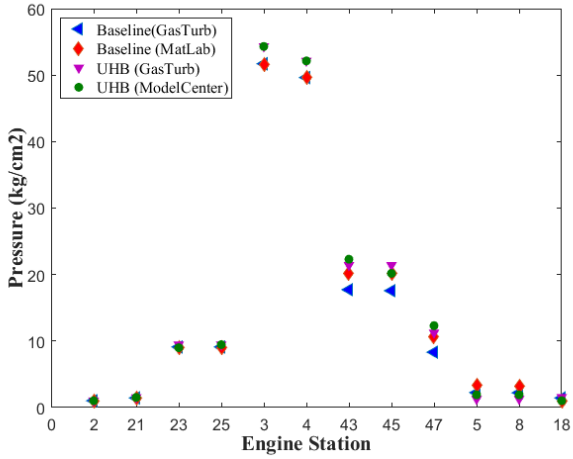

Figure 5 Pressures @ Engine Stations

Table 7 UHB DDSF Turbofan Engine Outputs

	Unit	GasTurb	ModelCenter	Error %
FN	*kN*	401.87	413.79	3.0
TSFC	*g/(kN s)*	6.84	6.34	7.3

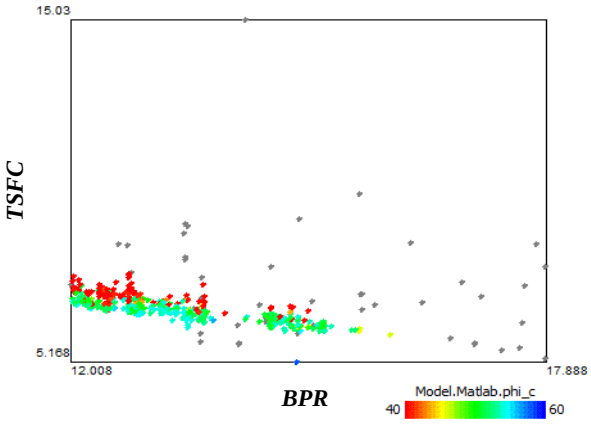

Figure 6 Scatter Plot (*TSFC vs BPR*)

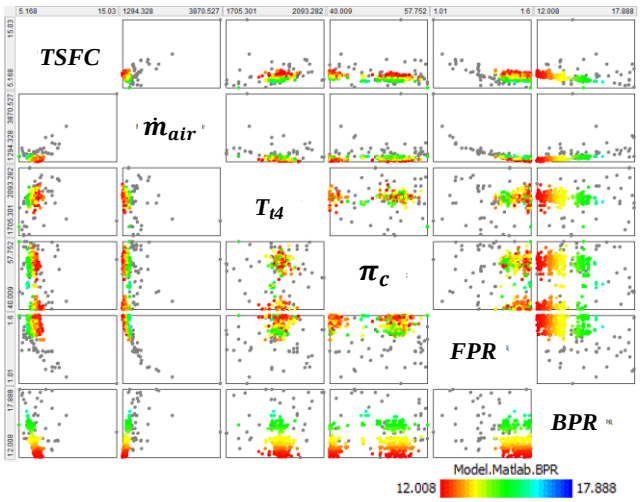

Figure 7 Scatter Matrix

Figure 7 is a scatter matrix, which is useful to understand the impacts of several important engine design parameters on the engine performance. It visualizes that TSFC of UHB DDSF turbofan engine has strong relationships with T_{t4}, π_c, FPR, andBPR. Similar to TSFC, $\dot{m}_{air}$ is also strongly correlated with those design variables. However, the data points shown in the BPR~FPR plot are scattered over the range and this implies the weak coupling between those two variables. Looking at the frontier front, it is clear that the higher the BPR, the lower the TSFC as discussed in numerous studies.

Despite there have been growing parametric studies on turbofan engines, it could be argued that there have been few studies about which engine design variable is relatively more sensitive to a certain engine performance. Having that said, the design and optimization model created in ModelCenter for this study provides a superior opportunity to investigate this issue.

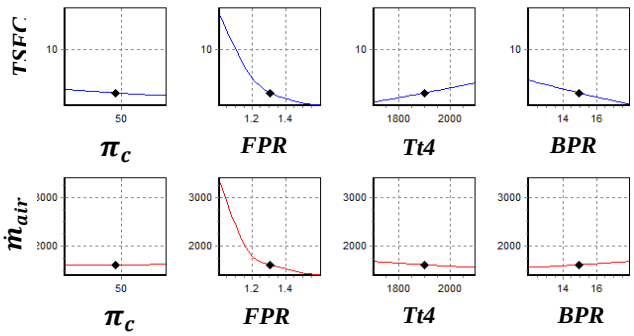

Figure 8 Prediction Profiler

For example, Figure 8 is a prediction profiler. This is one of the most respected methods to understand the sensitivity of variables or parameters. It reveals that increase of FPR and BPR reduces TSFC and TSFC is more sensitive to FPR than BPR. In case of $\dot{m}_{air}$, it is not considered sensitive to changes of π_c although it is dominantly affected by FPR similar to TSFC case.

Figure 9 is a sensitivity summary as called in ModelCenter. This visualizes which design variable impacts the objective functions more during the optimization process, and this can be generated with just a few clicks in the model by letting ModelCenter analyze the data gathered during the engine optimization. As shown in the figure, BPR has the biggest positive impact on TSFC. The figure also exhibits $\dot{m}_{air}$ is impacted mostly by both BPR and FPR at similar significant level. Now we recall that $\dot{m}_{air}$ of the derivative engine is not changed that much comparing to the baseline engine even if BPR is increased by 59.1%. To minimize TSFC, BPR is inevitably increased but this eventually increases $\dot{m}_{air}$. However, this is not the desired shape of a derivative engine since it implies the engine requires larger inlet area thus larger engine diameter. To prevent this situation, FPR as well as T_{t4} also need to be increased because those help to reduce the required air mass flow rate. This information can give engine scientists formidable intuition for variable handlings during the conceptual design stage.

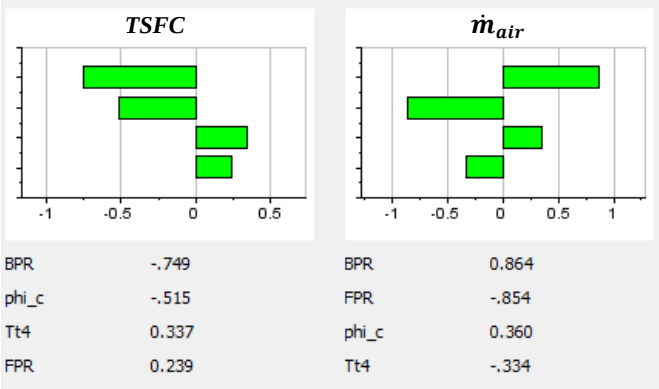

Figure 9 Sensitivity Summary

CONCLUSIONS

This study was an attempt to develop an optimized engine cycle of a derivative three spool UHB DDSF turbofan engine from an existing engine. To accomplish this goal, a baseline engine model was created in MatLab borrowing a data set from a reference [1] and it was validated with GasTurb 12. This engine model was implemented in ModelCenter and, finally, the model was linked to an optimization algorithm to complete a seamless design and optimization environment.

One main question was how the model could be set up for cycle development and optimization for a 'derivative' engine retaining the HP system of the original engine. This question was answered by keeping the area ratio of the HP compressor inlet and outlet constant. This area ratio could be recast as thermodynamic relationships like equation (18) which is premised on assumptions that the axial flow velocity is approximately constant and the mass is conserved through the HP compressor and this concept was coded in the baseline engine model.

The model has proven its capability. It configured the optimized engine cycle by improving TSFC (21.2%) while

minimizing the engine diameter in term of air mass flow rate to reduce nacelle drag and meet the airplane height requirement. The other engine outputs were found valid and well in line with the general behavior of turbofan engines.

One more advantage that engine scientists can expect from this method is that it enables parametric studies and sensitivity studies with various data analysis tools and plot options with minimum effort. Primarily, sensitivity studies visualized the relative significance of the design variables on each engine performance factor that has been treated in just few engine parametric studies.

NOMENCLATURE

A	area ratio
BPR	Bypass Ratio
F	thrust force
FPR	Fan Pressure Ratio
M	Mach number
P	pressure
R	gas constant
T	temperature
$TSFC$	thrust specific fuel consumption
V	velocity
a	speed of sound
e	polytrophic efficiency
g	gravity constant
$\dot{m}$	mass flow rate
π	total pressure ratio
τ	total temperature ratio
τ_λ	enthalpy ratio
c_p	specific heat at constant pressure
γ	specific heat ratio
η	isentropic efficiency

Subscripts

Arabic number	engine station
b	burner
c	compressor
cn	core nozzle
d	duct
f	fan, fuel-air ratio
fn	fan nozzle
h	heating value, high
i	intermediate
l	low
m	mechanical
p	pressure
r	free stream
t	turbine

REFERENCES

[1] AIAA, "An ultra-High Bypass Ratio Turbofan Engine for the Future," Request for Proposal, AIAA, 2014

[2] Selcuk Can Uysal, "High By-pass Ratio Turbofan Engines Aerothermodynamic Design and Optimization," Thesis, Feb. 2014

[3] Kalyanmoy Deb, et. al., "A Fast and Elitist Multiobjective Genetic Algorithm," IEEE Transactions on Evolutionary Computation, Vol. 6, NO.2, Apr. 2002

[4] A. Homaifar, et. al., "System Optimization of Turbofan Engines using Genetic Algorithm," App'. Math. Modeling, Vol. 18, NO.2, Feb. 1994

[5] PHOENIX INTEGRATION, ModelCenter, http://www.phoenix-int.com/modelcenter/integrate.php

[6] Jack D. Mattingly, et. al., "Elements of Propulsion: Gas Turbines and Rockets," AIAA Education Series, 2006

[7] HIH Saravanamuttoo, et. al., "Gas Turbine Theory, 6th Ed", Pearson Education Limited, 2008